Study on Seismic Damage Mode and Key Construction Damage Mechanism of Highway Pile-Plate Structure

Xiaoming Liu$^{(\boxtimes)}$ and Feng Xue

Anhui Transportation Holding Construction Management Co., Ltd., Hefei 241199, China
1398833475@qq.com

Abstract. The seismic design concept based on performance for bridge structures is an important direction for the continued improvement and development of bridge seismic design specifications. One of the key aspects is to choose reasonable indicators for defining and quantifying the seismic performance level of bridge structures. In this article, the Incremental Dynamic Analysis (IDA) method was used to simulate the entire earthquake damage and failure process of a rigid frame bridge with a high pier. The findings reveal that, in sleeve-type and bolted-type connection pile-plate structures under far-field and near-field seismic motions, different prefabricated pile positions and joints carry the same seismic force during the earthquake process. However, under far-field and near-field earthquakes, the state of the prefabricated pile pile bottom and connection structure differs under different Peak Ground Acceleration (PGA) levels.

Keywords: Seismic performance of bridge structures · high-pier rigid-frame bridge · panel pile structure · earthquake analysis

1 Introduction

In the context of current road construction, land resources continue to become increasingly scarce. The contradiction between the lack of available land and soil is extremely prominent. As a result, pile-plate roadbed has emerged as a new type of pile-plate beam structure, consisting of prefabricated plate beams and pipe piles as part of its framework system. Initially, pile-plate roads were mainly used in the field of railways. However, with technological advancements and innovative developments in construction techniques, pile-plate structures have since been widely applied in both the expansion and widening of highways, as well as in new construction projects [1–3]. Midas was used by Zhu Jun [4] to establish an entire model of the pile-plate roadbed. While selecting fatigue analysis points and analyzing the pile-top influence surface, preliminary calculations of the pile-plate connection fatigue performance were conducted. Zheng Wucong [5] explored various multi-scale modelling methods for pile-plate roadbeds in highways. By establishing multiple connection methods including CERIG connection, RBE3 connection, MPC method and common node coupling method, beam elements,

plate elements and solid elements could be connected through different ways to construct multi-scale models. Lei Jin [6] established a nonlinear finite element model of the pile-plate connection construction based on the engineering design example of this research project and using ANSYS finite element software.

The present study focuses on the pile-plate structure of a certain highway and aims to establish a nonlinear finite element model of the structure for seismic analysis.

2   Project Overview

The pile plate connection with the pre-stressed tube pile has a regular circular cross-section, with a diameter of 516 mm for the pile plate connection structure. The steel casing has a thickness of 8 mm. It is divided into two non-linear beam-column units along the height. The hoop reinforcement uses 10 mm HPB300 steel bars, and the longitudinal reinforcement uses 12 HRB400 steel bars with a diameter of 25 mm. The internal grouting material uses C50 compensating shrinkage concrete. The pre-stressed tube pile has a diameter of 500 mm and a height of 10 m. It is divided into 8 non-linear beam-column units along the height. The hoop reinforcement uses 10 mm HPB300 steel bars, and the longitudinal reinforcement uses 12 Φ25 mm bars for the filling section. The longitudinal reinforcement of the prefabricated pile uses 12 Φ12 mm and 12 pre-stressed steel bars with a diameter of 12.6 mm. The effective pre-pressure stress of concrete is 6 Mpa.

3   Establish a Finite Element Model of the Sheet Pile Structure

This paper presents the use of OpenSees software to create a nonlinear finite element model of the sheet pile structure and to conduct seismic analysis as shown in Fig. 1. The pile-plate connection structure has a steel casing thickness of 8 mm and its concrete grade is C50 to account for the constraining effects of the steel casing. The confinement concrete model of the steel pipe concrete is referenced. The material for the pre-stressed tube pile is C80 high-strength concrete, and its material model adopts the Kent-Park model due to its clear physical meaning, numerical stability, and ability to consider the stiffness degradation of concrete when subjected to repeated loads. The Steel02 model is employed in this study to simulate the steel casing, ordinary reinforcement, and pre-stressed reinforcement. The kinematic hardening rule with isotropic hardening in the tensile and compressive directions is adopted for all types of steel. Pre-stressing is applied by using the initial stress method. HRB400 steel bars and Q245 steel are used for the steel reinforcement and steel casing material, respectively.
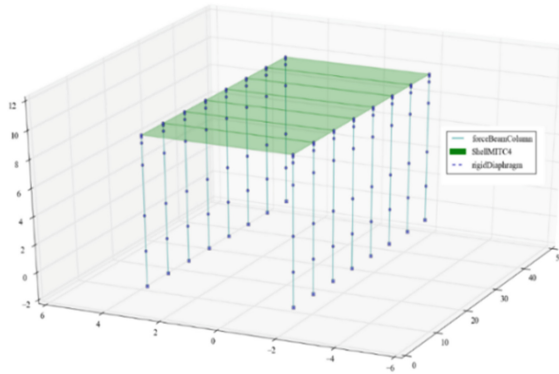
Fig. 1. OpenSees Finite Element Model.

4 Result Analysis

By selecting seismic waves from far and near fields, dynamic elastic-plastic time-history analysis of the sheet pile structure is conducted with increasing PGA to obtain a response of the entire failure process of the structure from the initial elastic state to gradual degradation and collapse. The bending moment-curvature changes of the pile bottom and joint positions, as well as the damage mechanisms of the protective layer concrete, core concrete, and longitudinal reinforcement strain, are analyzed. The analysis is carried out at three representative PGA-states of 0.3 g, 0.6 g and 0.9 g for the pile bottom of the prefabricated pile.

At PGA = 0.3 g, the bending moment curvature diagram, longitudinal bars, and strain-time relationship table (Fig. 2 and Table 1) of the prefabricated pile's base demonstrate a significant non-linear relationship between the bending moment curvature and the bottom of the pile, confirming its entry into the yield plastic stage. The longitudinal bars at the bottom have gradually shifted from compression to tension, with a maximum tensile strain of 0.00068, still within the elastic range. The protective and core concrete experience maximum compressive strains of −0.00061 and −0.00047, respectively. Small, barely visible cracks have appeared on the concrete's surface. Similarly, the joints exhibit a linear relationship in the bending moment curvature (Fig. 2 and Table 1), indicating that the external steel casing enhances lateral restraint. The joints remain in the linear elastic stage, with a maximum tensile strain of 0.00016 in the joints' longitudinal bar, while the steel bars primarily remain elastic. The core concrete shows a maximum compressive strain of −0.00027, indicating that the joint concrete remains in the elastic stage and has not reached the plastic stage.
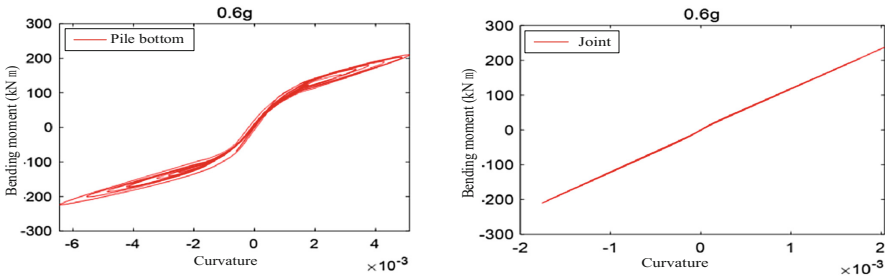
Under PGA = 0.6 g, the bending moment curvature diagram, longitudinal bars, and strain-time relationship table (Fig. 3 and Table 1) at the bottom of the prefabricated pile show that the bottom of the pile has entered the plastic yield stage. The longitudinal bars at the bottom exhibit a maximum tensile strain of 0.00178, nearing the yield stage. The maximum compressive strains of the protective concrete and core concrete are −0.001 and −0.00072, respectively, with visible surface cracks indicating minor damage. Similarly, the joints' relationships (Fig. 3 and Table 1) suggest that the bending moment
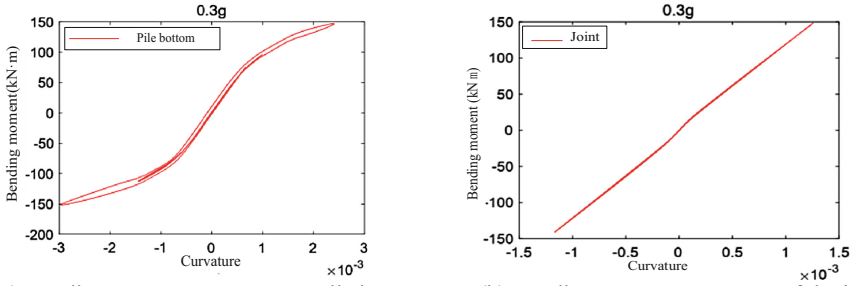
(a) Bending moment curvature at pile bottom

(b) Bending moment curvature of the joint.

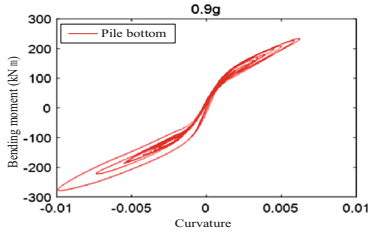**Fig. 2.** Mechanical performance at PGA $= 0.3$ g

curvature remains linearly related, indicating a linearly elastic state under PGA $= 0.6$ g. The joints' longitudinal bar experiences a maximum tensile strain of 0.00027, while the steel bars primarily remain in the linear elastic stage. The core concrete experiences a maximum compressive strain of -0.00043, and the joint concrete remains fundamentally intact.
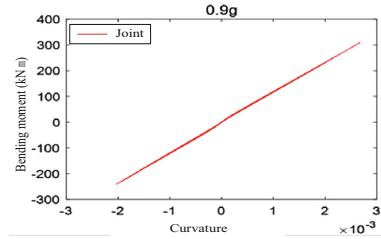

(a) Bending moment curvature at pile bottom

(b) Bending moment curvature of the joint.

Fig. 3. Mechanical performance at PGA $= 0.6$g

Under PGA $= 0.9$ g, the bending moment curvature relationship diagram, longitudinal steel bars, and strain-time relationship diagram for the protective and core concrete of the prefabricated pile were investigated (Fig. 4 and Table 1). The results revealed that the pile bottom experienced plastic yielding stages, with a maximum tensile strain of 0.00295 in the longitudinal steel, indicating yielding. The maximum compressive strains of the protective layer and core concrete were -0.00138 and -0.00091, respectively. Surface cracks in the concrete continued to propagate, resulting in mild damage. Similarly, the analysis of joint behavior under similar conditions (Fig. 4 and Table 1) showed that the bending moment curvature of the joint remained linear under PGA $= 0.9$ g. The joint remained in the linear elastic stage, with a maximum tensile strain of 0.00036 in the longitudinal rebar, indicating the steel bars were still in the linear elastic stage. The maximum compressive strain of the core concrete was -0.00055, and the joint concrete exhibited minimal or no damage.
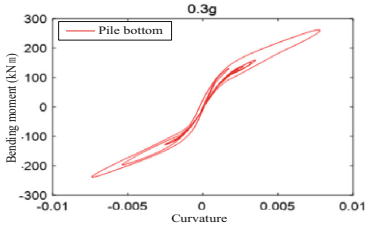
(a) Bending moment curvature at pile bottom

(b) Bending moment curvature of the joint.

Fig. 4. Mechanical performance at PGA = 0.9g

Table 1. Strain-time relationship table under different PGAs in the far-field condition.
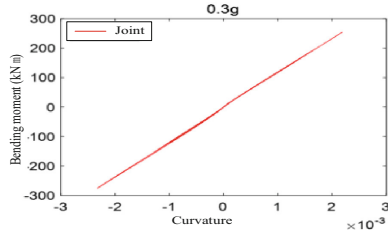
PGA(Unit: g)	The bottom of the prefabricated pile			The joint	
	Longitudinal bars	Protective layer concrete	Core concrete	Longitudinal bars	Core concrete
0.3	−0.00056	−0.00061	−0.00047	−0.00011	−0.00027
0.6	−0.00090	−0.00102	−0.00072	−0.000157	−0.00042
0.9	−0.00119	−0.00138	−0.00091	−0.000196	−0.00055

In the near-field region, the bending moment-curvature diagram, longitudinal reinforcement, and strain-time diagram of protective and core concrete at the bottom of prefabricated piles under PGA = 0.3 g indicate that the bottom of the piles has entered the plastic yielding stage. The maximum tensile strain in the longitudinal reinforcement is 0.0021, reaching the yield stage. The maximum compressive strains for the protective and core concrete are −0.00124 and −0.00087, respectively. Cracks gradually develop in the protective concrete, indicating mild damage. Similarly, the joint relationship reveals that the bending moment-curvature of the joint remains linear due to the reinforcing effect of the external steel sleeve. The joint remains in a linear elastic stage with a maximum tensile strain of 0.00030 in the longitudinal reinforcement. The steel bars remain in the linear elastic stage, while the maximum compressive strain in the core concrete is −0.00051. The joint concrete remains elastic and does not undergo plastic deformation (Fig. 5).

At PGA = 0.6 g, the bottom of the prefabricated piles entered the plastic stage. The longitudinal reinforcement reached a maximum tensile strain of 0.0061, indicating steel yielding. The protective and core concrete experienced maximum compressive strains of −0.00217 and −0.00129 respectively. The structure exhibited non-linear deformation with visible cracks and delamination in the protective concrete, resulting in moderate damage. However, the joint remained in a linear elastic state under the same conditions. The bending moment-curvature relationship of the joint remained linear, with a maximum tensile strain of 0.0005 in the longitudinal reinforcement. The steel in the joint maintained its linear elastic stage. The core concrete exhibited a maximum compressive strain of −0.00074, and there was no significant damage to the joint concrete (Fig. 6).
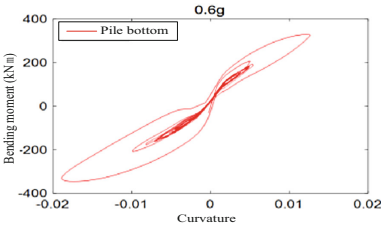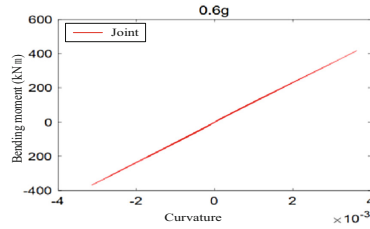
(a) Bending moment curvature at pile bottom   (b) Bending moment curvature of the joint.

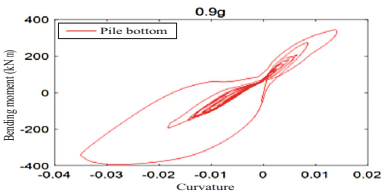**Fig. 5.** Mechanical performance at PGA = 0.3 g
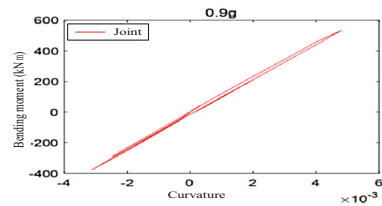

(a) Bending moment curvature at pile bottom   (b) Bending moment curvature of the joint.

Fig. 6. Mechanical performance at PGA = 0.6g

At PGA = 0.9 g, the bottom of the prefabricated pipe pile entered the plastic yielding stage. The longitudinal reinforcement exhibited a maximum tensile strain of 0.0118, indicating yielding. The protective layer concrete and core concrete experienced maximum compressive strains of −0.0035 and −0.0019 respectively. This led to the formation of a structural plastic hinge with wider cracks (at least 2 mm in width). The concrete in the entire plastic hinge area peeled off, resulting in severe structural damage. Conversely, the joint remained in a linear elastic state under the same conditions. The bending moment-curvature relationship of the joint remained linear, with a maximum tensile strain of the longitudinal reinforcement at 0.00067. The steel bar in the joint remained in the linear elastic stage, and the core concrete experienced a maximum compressive strain of −0.00097. Overall, there was minimal damage to the joint concrete (Fig. 7 and Table 2).

(a) Bending moment curvature at pile bottom   (b) Bending moment curvature of the joint.

Fig. 7. Mechanical performance at 0.9 g

Table 2. Strain-time relationship at various PGAs.

PGA(Unit: g)	The bottom of the prefabricated pile			The joint	
	Longitudinal bars	Protective layer concrete	Core concrete	Longitudinal bars	Core concrete
0.3	−0.00110	−0.00124	−0.00087	−0.000198	−0.00051
0.6	−0.00181	−0.00217	−0.00129	−0.000258	−0.00074
0.9	−0.00289	−0.00353	−0.00197	−0.000329	−0.000968

5   Conclusion

This paper analyzes the effects of far-field and near-field earthquake ground motions on highway pile-slab structures through time-domain analysis. The following conclusions can be drawn:

(1) Far-field earthquakes gradually damage prefabricated pipe piles with increasing PGA. At 0.1 g, the pile is elastic. At 0.2 g, plastic deformation starts, and at 0.3 g, cracks appear. At 0.7 g, bars yield and cracks widen. Up to 1.0 g, slight damage occurs. Connections remain undamaged due to steel reinforcement.

(2) Near-field earthquakes cause progressive damage to prefabricated pipe piles. At 0.1 g, the pile remains elastic. At 0.3 g, plastic deformation starts, yielding reinforcement and developing cracks. At 0.6 g, non-linear deformation occurs with visible cracks and peeling, causing moderate damage. At 0.9 g, severe damage arises with plastic hinges and wide cracks. Connection structures exhibit minimal damage due to steel casing restraint, even at PGA = 1.0 g.

References

1. Wang, H., Liu, W., Huang, X.: Comparative Research and Analysis of Prefabricated Buildings and Cast-in-Place Buildings. Special Materials Compilation of Industrial Architecture Magazine (2017)
2. Fang, Z., Dou, W., Zhang, H.: Seismic performance analysis of pile-plate roadbed structure. Anhui Archit. **28**(12), 136–138 (2021)
3. Tao, C.: Roadbed detection technology and its application. Constr. Technol. (23), 101–104 (2016)
4. Jun, Z., Nan, D.: Fatigue performance analysis of pile-plate connection joints for pile-plate roadbed. Eng. Constr. **32**(05), 673–675 (2018)
5. Zheng, W.: Study on Characteristics of Pile-Plate Roadbed Structure Based on Multiscale Finite Element Model. Hefei University of Technology (2018)
6. Jin, L.: Nonlinear finite element analysis of highway pile-plate structure connection structure based on ANSYS. Eng. Constr. **33**(05), 780–782 (2019)